Development of a Position Control System for Wheeled Humanoid Robot Movement Using the Swerve Drive Method Based on Fuzzy Logic Type-2

Bhakti Yudho Suprapto*, Suci Dwijayanti, Djulil Amri
Department of Electrical Engineering, Sriwijaya University,
Palembang-Prabumulih Street KM. 32 Inderalaya, South of Sumatera, Indonesia
**bhakti@ft.unsri.ac.id; sucidwijayanti@ft.unsri.ac.id; djulilamri@ft.unsri.ac.id*

***Abstract*—A humanoid robot is capable of mimicking human movements, which poses a challenge for researchers. This has led some to utilise wheels to facilitate its motion. However, achieving smooth and accurate movements at desired positions remains a challenge, necessitating the development of an optimal control system and movement method. In this study, solutions to address these challenges include the use of type-2 fuzzy logic controller (FLC) and the swerve drive method. During the steering rotation movement testing, type-1 FLC exhibits the fastest response time of 0.8 seconds, but oscillations occur, reaching up to 117 degrees to achieve the set point of 90 degrees. Additionally, type-1 FLC cannot reach the set point of -90 degrees. On the contrary, type-2 FLC aligns successfully with both set points of 90 and -90 degrees. In coordinate movement testing, type-1 FLC still shows an error between 1 cm and 2 cm compared to type-2 FLC, particularly with 3 and 5 members, which are equal to the given set point. The results of the tests indicate that type-2 FLC is reliable, showing a small steady-state error, stability, and no overshoot, despite its longer response time and processing duration compared to type-1 FLC.**

***Index Terms*—Humanoid robot; Movement; Swerve drive method; Type-2 FLC; Type-1 FLC.**

I. INTRODUCTION

The development of robot technology has been a major highlight in recent decades, bringing about amazing innovations and changing paradigms in various industries. Robots are no longer just simple automated machines, but entities that are increasingly complex and intelligent. One of the latest trends is the development of humanoid robots that mimic the body structure and physical abilities of humans. These robots can perform not only physical tasks like humans but can also interact and communicate with their surroundings. However, designing a humanoid robot that can move like a human using legs presents a significant challenge. To overcome this problem, wheels are usually used as the robot's propulsion system [1]. Mecanum wheels and others are commonly utilised to allow free movement. However, their relatively high cost requires research into alternative solutions, such as the combination of gears and motors, known as the swerve drive method [2]–[6]. This method features a simple design and the ability to provide omnidirectional mobility [7].

The swerve drive is a uniquely designed propulsion system that allows the robot to pivot while moving through any terrain [4]. Each wheel rotates on a vertical axis, allowing for exceptional manoeuvrability [8]. The mounts for the steering drive can pivot and pan independently and can even rotate while the robot is moving in a straight line. The swerve drive method is not only used in robots [6], [8], [9] but also used to facilitate manoeuvring in trolleys [10], hospital beds [7], and autonomous vehicles [11]–[13]. Movement and position using this swerve drive also require optimal control. Several controllers, such as cascade proportional integral derivative (PID) used in balancing robots [14], improved particle swarm optimisation (PSO) with base proportional integral derivative (PID) in nonlinear hydraulic system position control systems [15], and intelligent algorithms like fuzzy logic [16], fuzzy logic and PID for robot movement [17], and adaptive neuro fuzzy for controlling the position of industrial robots [18], have been widely studied.

Fuzzy logic operates on the basis of the principles of logic and utilises a reasoning approach that resembles human decision-making processes. It handles uncertainty by employing a knowledge foundation expressed through intuitive linguistic rules. Fuzzy logic does not rely on complex mathematical models to solve problems, but it leverages the concept of uncertainty, typically seen as an attribute of information. Fuzzy reasoning allows for handling a significant amount of uncertainty and utilises type-1 fuzzy sets, representing uncertainty with values in the range [0, 1]. In situations where an entity is in an uncertain condition, such as in measurements, determining its precise membership value becomes challenging. In such cases, a type-1 fuzzy set may be less sensible than other types of fuzzy set. However, the use of accurate membership functions becomes impractical for dealing with uncertainty. Therefore, another type of fuzzy set is needed to handle such uncertainty, known as a type-2 fuzzy set.

Type-2 fuzzy sets can reduce the magnitude of uncertainty

Manuscript received 2 September, 2023; accepted 18 December, 2023.
This study was supported through the DIPA Universitas Sriwijaya according to the Research Contract No. 0096.015/UN9/SB3.LP2M.PT/2023 dated May 8, 2023.

in a system by better handling linguistic uncertainty and modelling the vagueness and unreliability of information [19]. Due to the advantages of type-2 fuzzy logic, many researchers use this controller to regulate the fluid process level in a tank [20], the mobile robot controller [19], and classification and pattern recognition [21].

In this study, type-2 fuzzy logic is used to control the movement of a wheeled humanoid robot using the swerve drive method. The main contribution of this study is the implementation of a fuzzy type-2 control system, allowing uncertainty modelling to achieve better movement and position control of humanoid robots, especially when compared to fuzzy logic.

The remainder of the paper is structured as follows. Section II describes the swerve drive method and kinematics. Section III offers a brief overview of the basic concepts of type-2 fuzzy systems. Section IV provides a method. Section V presents results and discussion. Finally, Section VI concludes the paper.

II. SWERVE DRIVE AND KINEMATICS

A. Swerve Drive

The swerve drive is a specialised propulsion wheel that can rotate around a vertical axis to adjust the direction of rotation of the wheel according to the desired kinematics [3]. Rotation around the vertical axis can be independently performed by each wheel without involving the others. Consequently, a robot equipped with a swerve drive as its propulsion system can change direction and execute movements simultaneously, resulting in highly flexible manoeuvres.

In the swerve drive, omnidirectional refers to the robot's ability to navigate freely in any direction at any given time. The swerve drive modules consist of two motors, a gearbox, encoders, and a wheel. One motor facilitates wheel rotation, while the other manages steering. The gearbox plays a crucial role in steering wheel movement and encoders determine the rotational position of the drive wheel. Although swerve drive systems are regarded as top-tier in the competitive robotics sphere, their adoption by average teams is hindered by both cost and complexity.

This challenge is applicable to any robotics team, particularly those facing limitations in funding or experience. The swerve drive is a distinctive propulsion wheel capable of rotating on the vertical axis to align the rotation direction of the wheel according to the desired kinematics. Each wheel can independently run a rotation around the vertical axis without affecting the others. Consequently, a robot equipped with a swerve drive can alter its direction and execute movements simultaneously, allowing for exceptionally flexible manoeuvres. Figure 1 shows an example of a swerve drive.

Individual wheels can rotate on the vertical axis without affecting the others. As a result, a robot equipped with a swerve drive can simultaneously alter its direction and move, allowing for flexible manoeuvres. To simulate the trajectory of a projectile during atmospheric flight, the widely recognised rigid-body dynamic model with six degrees of freedom (6-DOF) is employed [22]. This set of equations is collectively referred to as projectile linear theory [23]. Equations (1) to (6) represent the dynamic equations of the linear theory applicable to this analysis:

$$\begin{Bmatrix} \tilde{v}' \\ \tilde{w}' \\ \tilde{q}' \\ \tilde{r}' \end{Bmatrix} = \begin{bmatrix} -A & 0 & 0 & -D \\ 0 & -A & D & 0 \\ \frac{B}{D} & \frac{C}{D} & H & -F \\ -\frac{C}{D} & \frac{B}{D} & F & H \end{bmatrix} \begin{Bmatrix} \tilde{v} \\ \tilde{w} \\ \tilde{q} \\ \tilde{r} \end{Bmatrix} + \begin{Bmatrix} V_F \\ W_F \\ Q_F \\ R_F \end{Bmatrix} \tag{1}$$

$$Q' = \frac{D}{V}\tilde{q}, \tag{2}$$

$$\varphi' = \frac{D}{V}\tilde{r}, \tag{3}$$

$$x' = D, \tag{4}$$

$$y' = \frac{D}{V}\tilde{v} + \varphi D, \tag{5}$$

$$z' = \frac{D}{V}\tilde{w} - \theta D. \tag{6}$$

Fig. 1. Swerve drive model [3].

The nondimensionalised arc length, denoted as $\boldsymbol{s}$, serves as the independent variable in the dynamic equations of projectile linear theory. As indicated in (7), the arc length is directly proportional to the time

$$\boldsymbol{s} = \frac{\mathbf{1}}{\boldsymbol{D}}\int_0^t \boldsymbol{V}\boldsymbol{dt}. \tag{7}$$

The prime notation in (1) to (6) means that the derivatives are computed with respect to the dimensionless arc length rather than the time. Additionally, the linear theory equations adopt a reference frame aligned with the projectile's axis of symmetry, but without any rolling motion. Variables in this reference frame, also referred to as the fixed-plane frame or the no-roll frame, are denoted by a tilde superscript. A single-axis rotation around the projectile's axis of symmetry establishes the connection between the no-roll frame and the body-fixed frame used in traditional 6-DOF equations. Analysis of essential swerve responses due to control inputs disregards the effects of gravity and atmospheric winds.

B. Forward Kinematics

Forward kinematics is the systematic procedure for computing the position of an object, such as a robot, to determine its destination position based on its current location [24], [9]. Its purpose is to measure the displacement that the robot underwent from its initial position to its current position. In this study, a rotary encoder functions as a sensor,

supplying data on the robot's location by computing its angular velocity. These data are then used as input for forward kinematic computations to derive the values of the X- and Y-coordinates, along with the direction the robot is facing, according to the following equation

$$\begin{bmatrix} \dot{x} \\ \dot{y} \\ \dot{\omega} \end{bmatrix} = \begin{bmatrix} -\sin(\omega+\alpha_1) & \cos(\omega+\alpha_1) & 2R^{-1^T} \\ -\sin(\omega+\alpha_2) & \cos(\omega+\alpha_2) & 2R^{-1} \\ \vdots & \vdots & \vdots \\ -\sin(\omega+\alpha_n) & \cos(\omega+\alpha_n) & 2R^{-1} \end{bmatrix} \begin{bmatrix} V_{W(1)} \\ V_{W(2)} \\ \vdots \\ V_{W(n)} \end{bmatrix}. \quad (8)$$

In (8), ẋ represents the X-coordinate of the robot, ẏ denotes the Y-coordinate of the robot, $\dot{\omega}$ signifies the direction the robot is facing, α stands for the angle of orientation of the rotary encoder, ω indicates the direction the robot is facing according to the reading of the gyroscope sensor, R represents the distance from the omni wheel to the centre point of the robot, and $V_{W(n)}$ is the linear velocity of the rotary encoder.

C. Inverse Kinematics

Inverse kinematics is the reverse process of forward kinematics. In this approach, the destination position is initially provided, followed by a mathematical calculation to obtain the required output values required to reach that destination position. In this case, the destination position is related to the robot's velocity [8]. This study specifically employs inverse kinematics for the swerve drive, as depicted in Fig. 2.

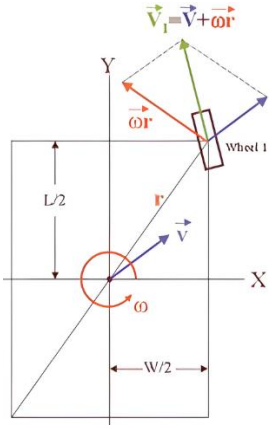

Fig. 2. Inverse kinematics.

In Fig. 2, it is evident that the translational speed of the robot on a wheel ($\tilde{v}_1$) is the vector addition of the robot's translational velocity ($\tilde{v}$) and rotational velocity (ω). To determine the values of the X-axis and Y-axis, the formulation is expressed in (9) and (10), where $\tilde{v}_x$ represents the robot's translational velocity on the X-axis and $\tilde{v}_y$ represents the robot's translational velocity on Y-axis:

$$\tilde{v}_x = V_x + \frac{\omega L}{r}, \quad (9)$$

$$\tilde{v}_y = V_y + \frac{\omega W}{r}. \quad (10)$$

After obtaining the translational velocity values along the X-axis and Y-axis, the speed of a wheel and the steering angle can be computed using (11) and (12):

$$\text{velocity} = \sqrt{\tilde{v}_x^2 + \tilde{v}_y^2}, \quad (11)$$

$$\text{angle} = \tan^{-1}\left(\frac{\tilde{v}_x}{\tilde{v}_y}\right). \quad (12)$$

III. Fuzzy Logic Type-2

Because the distinction between type-2 and type-1 is related to the nature of the membership functions [21], the structure of type-2 fuzzy rules is the same as that of type-1. Consequently, the only difference lies in the fact that some or all of the fuzzy sets used in the rules are now type-2. In a type-1 fuzzy system with type-1 fuzzy output sets, we perform defuzzification to obtain a number that is a crisp (type-0) representation of the combined output sets. However, in the type-2 situation, where the output sets are type-2, expanded versions of type-1 defuzzification procedures must be utilised [21], [25].

When a type-1 membership function is blurred to the left and right, as shown in Fig. 3, a type-2 membership function is formed. In this scenario, for a given value x^1, the membership function u^1 returns different values that are not all equally weighted, allowing us to assign membership grades to all of those points.

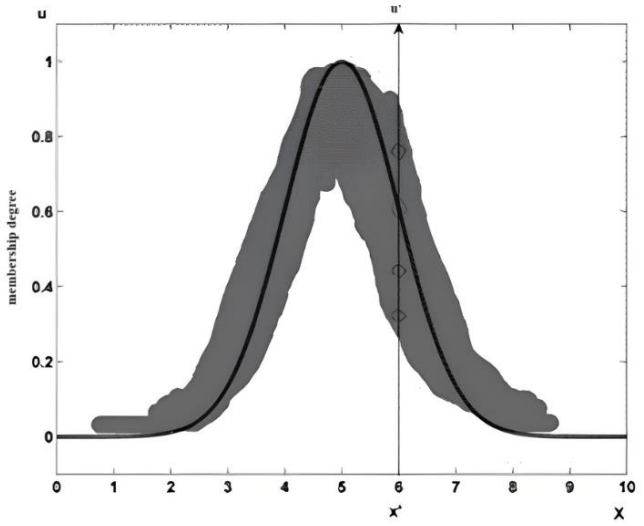

Fig. 3. The type-2 membership function is a muddled version of the type-1 membership function.

A three-dimensional membership function, or type-2 membership function, is created by executing this for every $x \in X$, describing a type-2 fuzzy set. The membership function of a type-2 fuzzy set Ā is as follows

$$\bar{A} = \left\{\left((x,u), \mu_{\bar{A}}(x,u)\right) \forall x \in X, \forall u \in J_x \subseteq [0,1]\right\}, \quad (13)$$

in which $0 \le \mu_A(x, u) \le 1$. In fact, $J_x \subseteq [0,1]$ represents the primary membership of x, and $\mu_A(x, u)$ is a type-1 fuzzy set known as the secondary set. Therefore, the main membership for a type-2 membership grade can be any subset in [0, 1]. For every primary membership, there is a secondary membership that defines the possibilities of the primary membership and can also be in [0, 1]. The footprint of uncertainty (FOU) is a region that represents uncertainty. But if $\mu_A(x, u) = 1$, $\forall u \in$

$J_x \subseteq [0, 1]$, there is an interval type-2 membership function, as shown in Fig. 4. The interval type-2 fuzzy set is represented by the uniform shading for the FOU, which may be explained by an upper membership function $\mu_A(x)$ and a lower membership function $\mu_A(x)$.

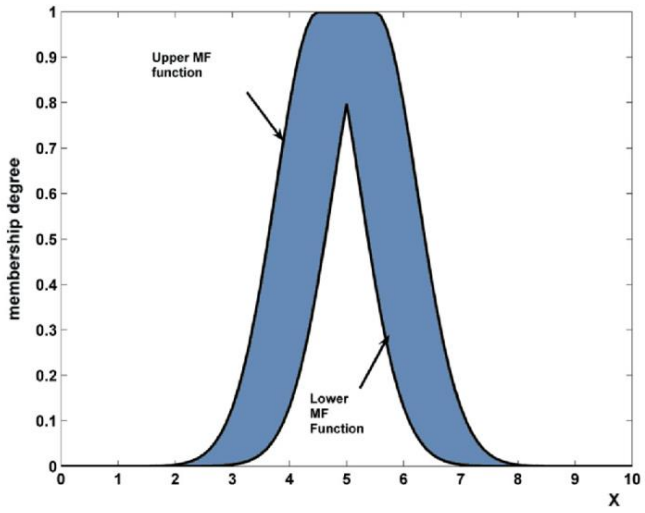

Fig. 4. Interval type-2 membership function.

A fuzzy logic system (FLS) that uses at least one type-2 fuzzy set is referred to as a type-2 FLS. FLSs of type-1 are incapable of directly managing uncertainty in rules, relying on particular type-1 fuzzy sets fully characterised by singular numerical values. In contrast, type-2 fuzzy logic systems (FLSs) are beneficial in situations where establishing a precise numerical membership function is challenging and there are uncertainties in measurements. Fuzzy logic type-2 is an enhancement of uncertainty calculations in the overall fuzzy logic process and has the ability to handle uncertainty that fuzzy logic type-1 does not possess. The processing block of fuzzy logic type-2 is generally depicted in Fig. 5.

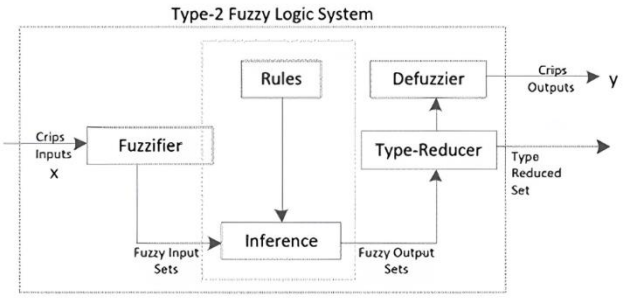

Fig. 5. Block of type-2 fuzzy logic processing [26].

IV. METHOD

A. Hardware System Design

The mechanical configuration of a robot significantly affects its range of motion. The research focussed primarily on the hardware system design of the humanoid robot, specifically the propulsion mechanism. This involved designing and implementing wheels on the robot's legs to facilitate its movement and repositioning. A wheel drive system with a swerve drive model was developed to enhance the navigation and manoeuvrability of humanoid robots, as depicted in Fig. 6.

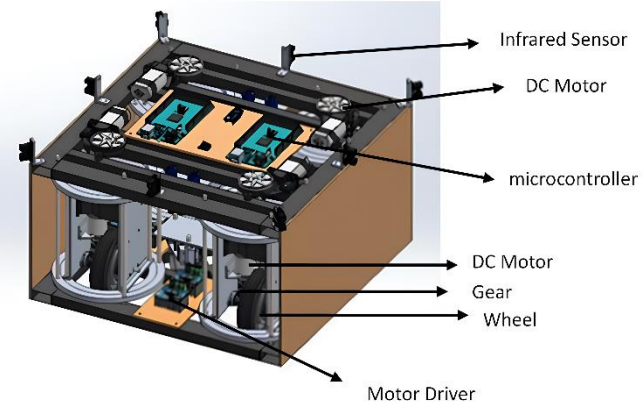

Fig. 6. Swerve drive design.

B. Software System Design

This study develops a software system for the humanoid robot that enables it to achieve stable and precise navigation while moving. The software system involves programming the humanoid robot and developing a mathematical control system for it. The objective of this study is to create a programme that allows the humanoid robot to precisely relocate itself from one location to another. The algorithm used in the humanoid robot design is depicted in Fig. 7, while diagram blocks illustrating the robot's movement can be observed in Fig. 8.

The programme begins with the robot ascertaining its initial position value, namely the position before any movement, as shown in Fig. 7.

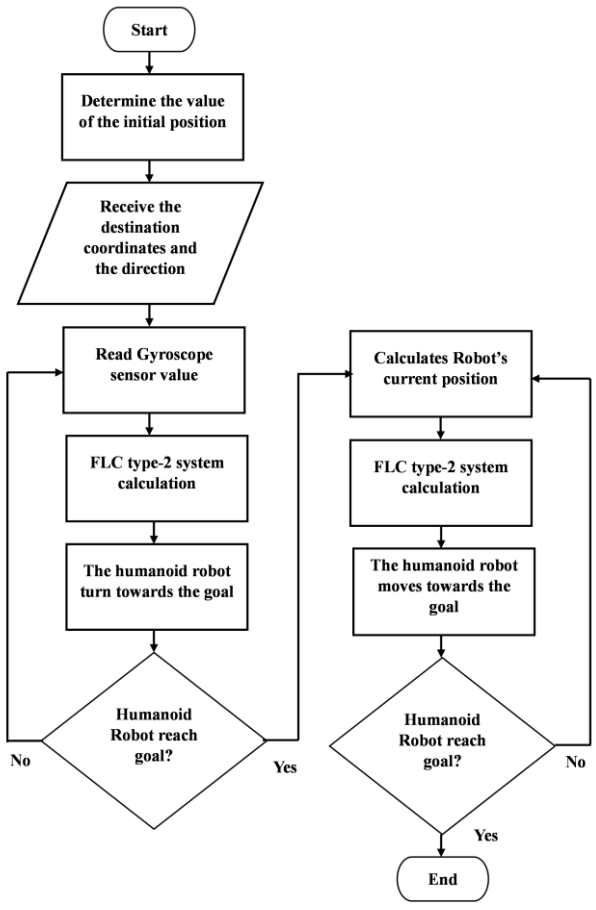

Fig. 7. Flow chart of robot movement design.

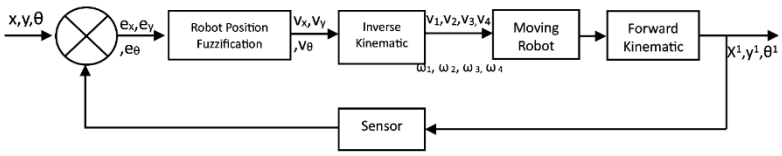

Fig. 8. Blocks of diagrams of the control system.

Additionally, the robot is provided with destination coordinate data and the preferred orientation. The robot adjusts its heading direction to align with the destination by first obtaining the gyroscope sensor reading, then using the type-2 fuzzy logic control (FLC) system to calculate the necessary adjustments, and finally executing the turn towards the target. Once the target is reached, the robot proceeds to the next destination by determining its current position and using the FLC system for navigation. The robot continues its movement until it reaches the intended place, and so on.

The robot movement can be observed in Fig. 8. The values x, y, and θ represent the desired destination or set point. Specifically, x represents the distance required to reach the destination along the X-coordinate, y represents the distance required along the Y-coordinate, and θ represents the direction towards the robot. Subsequently, the values of x, y, and θ undergo a transformation into fuzzy membership functions. Consequently, the output of the type-2 FLC system is then utilised in the inverse kinematic computation to provide the speed of each wheel (v_1, v_2, v_3, v_4) and the steering angle of each wheel (ω_1, ω_2, ω_3, ω_4). The robot uses these values to execute motions in varying positions, determining its new position through forward kinematic computations. The control system operates on a closed-loop concept, with feedback obtained from two sensors: the proximity sensor and the gyroscope sensor.

V. Results and Discussion

The study yielded several results, including the completion of the physical design of the hardware of the wheeled humanoid robot, specifically the swerve drive wheels for the driving mechanism. Additionally, the study involved developing a fuzzy logic control system and testing it on the movement of the robot. The hardware design was implemented using the preexisting three-dimensional architecture depicted in Fig. 6. Activities in the hardware design included tasks such as procuring hardware and materials, constructing the foundation of the swerving drive, installing various components, connecting them together, and conducting tests on the robot. The research resulted in swerving drive wheels, serving as the base and limbs of a wheeled humanoid robot, as depicted in Fig. 9.

Fig. 9. Swerve drive wheels.

A. Fuzzy Logic Control System Design

The control system in this study is composed of three inputs: the robot's X-coordinate movement, the robot's Y-coordinate movement, and the robot's rotational movement (heading). This study explored three conditions: the input condition with three membership functions, the input condition with five membership functions, and the input condition with seven membership functions. The membership functions examined in this study are presented in Table I for membership functions at XY-coordinates and Table II for membership functions at the heading.

TABLE I. THE MEMBERSHIP FUNCTION AT XY-COORDINATES.

3 Member	**Type-2 FLC**				**Type-1 FLC**	
	Upper		**Lower**			
	Lower Limit	**Upper Limit**	**Lower Limit**	**Upper Limit**	**Lower Limit**	**Upper Limit**
Negative	-550	-50	-450	-150	-500	-100
Zero	-200	200	-100	100	-150	150
Positive	50	550	150	450	100	500
5 Member	**Type-2 FLC**				**Type-1 FLC**	
	Upper		**Lower**			
	Lower Limit	**Upper Limit**	**Lower Limit**	**Upper Limit**	**Lower Limit**	**Upper Limit**
Negative Far	-550	-200	-450	-300	-500	-250
Negative Near	-350	0	-250	-100	-300	-50
Zero	-150	150	-50	50	-100	100
Positive Near	0	350	100	250	50	300
Positive Far	200	550	300	450	250	500
7 Member	**Type-2 FLC**				**Type-1 FLC**	
	Upper		**Lower**			
	Lower Limit	**Upper Limit**	**Lower Limit**	**Upper Limit**	**Lower Limit**	**Upper Limit**
Negative Far	-550	-250	-450	-350	-500	-300
Negative Normal	-400	-100	-300	-200	-350	-150
Negative Near	-250	0	-150	-100	-200	-50
Zero	-120	120	-20	20	-70	70
Positive Near	0	250	100	150	50	200
Positive Normal	100	400	200	300	150	350
Positive Far	250	550	350	450	300	500

TABLE II. THE MEMBERSHIP FUNCTION AT HEADING.

3 Member	Type-2 FLC				Type-1 FLC	
	Upper		Lower			
	Lower Limit	Upper Limit	Lower Limit	Upper Limit	Lower Limit	Upper Limit
Negative	-180	-27	-162	-63	-180	-45
Zero	-78	78	-42	42	-60	60
Positive	27	180	-63	162	45	180
5 Member	**Type-2 FLC**				**Type-1 FLC**	
	Upper		**Lower**			
	Lower Limit	**Upper Limit**	**Lower Limit**	**Upper Limit**	**Lower Limit**	**Upper Limit**
Negative Far	-180	-77	-162	-113	-180	-95
Negative Near	-123	-2	-87	-38	-105	-20
Zero	-53	53	-17	17	-35	35
Positive Near	2	123	38	87	20	105
Positive Far	77	180	113	162	95	180
7 Member	**Type-2 FLC**				**Type-1 FLC**	
	Upper		**Lower**			
	Lower Limit	**Upper Limit**	**Lower Limit**	**Upper Limit**	**Lower Limit**	**Upper Limit**
Negative Far	-180	-82	-162	-118	-180	-100
Negative Normal	-138	-32	-102	-68	-120	-50
Negative Near	-93	13	-57	-23	-75	-5
Zero	-43	43	-7	7	-25	25
Positive Near	-13	93	23	57	5	75
Positive Normal	32	138	68	102	50	120
Positive Far	82	180	118	162	100	180

The area of each member is determined by three domains based on the difference between the distance set point and the current distance value: negative (N), zero (Z), and positive (P). Regarding the membership functions with 5 and 7 members, the narrowing value of the three-member membership function is used to represent different conditions. Figures 10 and 11 show the membership functions in fuzzy logic type-2 based on the number of membership functions for XY- coordinates and heading.

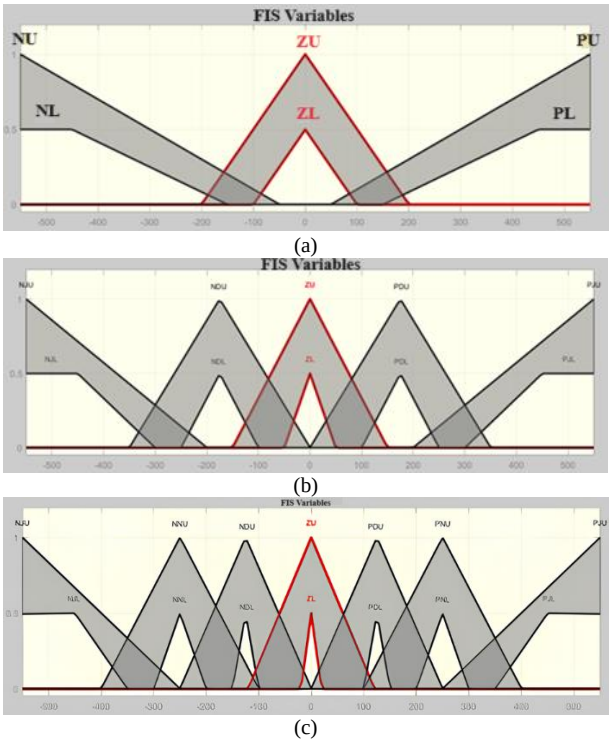

(a)

(b)

(c)

Fig. 10. The membership function at XY-coordinates: (a) 3 membership function; (b) 5 membership function; (c) 7 membership function.

Both of the fuzzy logic control systems used in this research utilise two inputs, namely distance and velocity, based on the fuzzy rules shown in Tables III, IV, and V. The system generates output in the form of position movement, guiding the robot towards the target position.

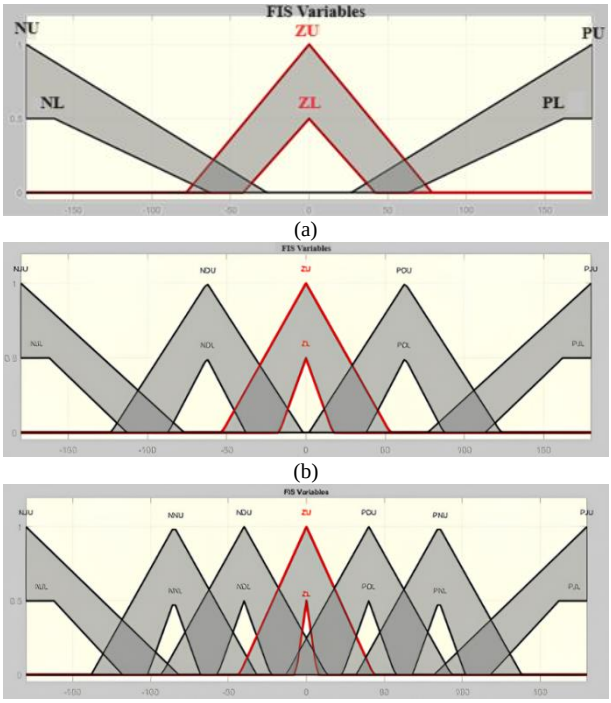

(a)

(b)

(c)

Fig. 11. The membership function at heading: (a) 3 membership function; (b) 5 membership function; (c) 7 membership function.

TABLE III. THE MEMBERSHIP FUNCTION RULES WITH 3 MEMBERS.

Rule	Input		Output
	Distance	Speed	Position Change
1	Negative	Negative	Negative Fast
2	Negative	Zero	Negative Slow
3	Negative	Positive	Negative Fast
4	Zero	Negative	Negative Slow
5	Zero	Zero	Very Slow
6	Zero	Positive	Positive Slow
7	Positive	Negative	Positive Fast
8	Positive	Zero	Positive Slow
9	Positive	Positive	Positive Fast

The distance input was derived by calculating the disparity

between the target distance and the current robot distance, while the velocity input was produced by measuring the rate of change of the distance function over time. The result of position movement in this study was represented by the pulse width modulation (PWM) value of each wheel, which was classified into five levels: Fast Negative, Slow Negative, Very Slow, Slow Positive, and Fast Positive. The results of this research are presented in Table VI.

TABLE IV. THE MEMBERSHIP FUNCTION RULES WITH 5 MEMBERS.

Rule	Input		Output
	Distance	Speed	Position Change
1	Negative Far	Negative Far	Negative Fast
2	Negative Far	Negative Near	Negative Slow
3	Negative Far	Zero	Very Slow
4	Negative Far	Positive Near	Negative Slow
5	Negative Far	Positive Far	Negative Fast
6	Negative Near	Negative Far	Negative Slow
7	Negative Near	Negative Near	Negative Slow
8	Negative Near	Zero	Very Slow
9	Negative Near	Positive Near	Negative Slow
10	Negative Near	Positive Far	Negative Slow
11	Zero	Negative Far	Very Slow
12	Zero	Positive Near	Very Slow
13	Zero	Zero	Very Slow
14	Zero	Positive Near	Very Slow
15	Zero	Positive Far	Very Slow
16	Positive Near	Negative Far	Positive Slow
17	Positive Near	Negative Near	Positive Slow
18	Positive Near	Zero	Very Slow
19	Positive Near	Positive Near	Positive Slow
20	Positive Near	Positive Far	Positive Slow
21	Positive Far	Negative Far	Positive Fast
22	Positive Far	Negative Near	Positive Slow
23	Positive Far	Zero	Very Slow
24	Positive Far	Positive Near	Positive Slow
25	Positive Far	Positive Far	Positive Fast

TABLE V. THE MEMBERSHIP FUNCTION RULES WITH 7 MEMBERS.

Rule	Input		Output
	Distance	Speed	Position Change
1	Negative Far	Negative Far	Negative Fast
2	Negative Far	Negative Normal	Negative Fast
3	Negative Far	Negative Near	Negative Slow
4	Negative Far	Zero	Very Slow
5	Negative Far	Positive Near	Negative Slow
6	Negative Far	Positive Normal	Negative Fast
7	Negative Far	Positive Far	Negative Fast
8	Negative Normal	Negative Far	Negative Fast
9	Negative Normal	Negative Normal	Negative Slow
10	Negative Normal	Negative Near	Negative Slow
11	Negative Normal	Zero	Very Slow
12	Negative Normal	Positive Near	Negative Slow
13	Negative Normal	Positive Normal	Negative Slow
14	Negative Normal	Positive Far	Negative Fast
15	Negative Near	Negative Far	Negative Slow
16	Negative Near	Negative Normal	Negative Slow
17	Negative Near	Negative Near	Very Slow
18	Negative Near	Zero	Very Slow
19	Negative Near	Positive Near	Very Slow
20	Negative Near	Positive Normal	Negative Slow
21	Negative Near	Positive Far	Negative Slow
22	Zero	Negative Far	Very Slow
23	Zero	Negative Normal	Very Slow
24	Zero	Negative Near	Very Slow
25	Zero	Zero	Very Slow
26	Zero	Positive Near	Very Slow
27	Zero	Positive Normal	Very Slow
28	Zero	Positive Far	Very Slow
29	Positive Near	Negative Far	Positive Slow
30	Positive Near	Negative Normal	Positive Slow
31	Positive Near	Negative Near	Very Slow
32	Positive Near	Zero	Very Slow
33	Positive Near	Positive Near	Very Slow
34	Positive Near	Positive Normal	Positive Slow
35	Positive Near	Positive Far	Positive Slow
36	Positive Normal	Negative Far	Positive Fast
37	Positive Normal	Negative Normal	Positive Slow
38	Positive Normal	Negative Near	Positive Slow
39	Positive Normal	Zero	Very Slow
40	Positive Normal	Positive Near	Positive Slow
41	Positive Normal	Positive Normal	Positive Slow
42	Positive Normal	Positive Far	Positive Fast
43	Positive Far	Negative Far	Positive Fast
44	Positive Far	Negative Normal	Positive Fast
45	Positive Far	Negative Near	Positive Slow
46	Positive Far	Zero	Very Slow
47	Positive Far	Positive Near	Positive Slow
48	Positive Far	Positive Normal	Positive Fast
49	Positive Far	Positive Far	Positive Fast

TABLE VI. THE OUTPUT VALUE OF THE FUZZY LOGIC SYSTEM.

Type-2 FLC		Type-2 FLC	
Member	PWM	PWM	
		Upper	Lower
Negative Fast	-175	-200	-175
Negative Slow	-125	-150	-125
Very Slow	(Set Point - Position) × 1.5	(Set Point - Position) × 1.5	(Set Point - Position) × 1
Positive Slow	125	150	125
Positive Fast	175	200	175

B. Testing of a Fuzzy Logic Control System on the Movement of a Wheeled Humanoid Robot

To demonstrate the performance of the humanoid robot in executing movements using the swerve drive method, its system is tested. The tests include turning the robot's facing direction, movement along the X-axis, and movement along the Y-coordinate. During motion system tests, the expectation is that the robot can achieve results wherein it moves toward the specified set point in a straight, stable, and accurate manner.

Figures 12, 13, and 14 depict the tests for 90, -90, and 180 degree steering rotation movements on type-2 FLC and type-1 FLC with 3, 5, and 7 members.

Based on Fig. 12, it is observed that, for a rotation of 90 degrees, all members can reach the desired set point. Type-1 FLC with 3 members exhibits the fastest response, namely 0.8 seconds, but oscillations occur, reaching 117 degrees. In terms of stability, type-2 FLC with 5 members is more stable. However, for a rotation of -90 degrees, as seen in Fig. 13, none of the members in type-1 FLC align with the set point, resulting in a steady-state error of 4 degrees. Despite this,

type-1 FLC has the fastest response. Moving on to a rotation of 180 degrees, in Fig. 14, the fastest response is with type-1 FLC at 0.9 seconds, but it exhibits the highest oscillation, reaching 243 degrees. On the contrary, type-2 FLC shows better stability and steady-state error. Overall, type-2 FLC exhibits better control accuracy compared to type-1 FLC in steering rotation movements.

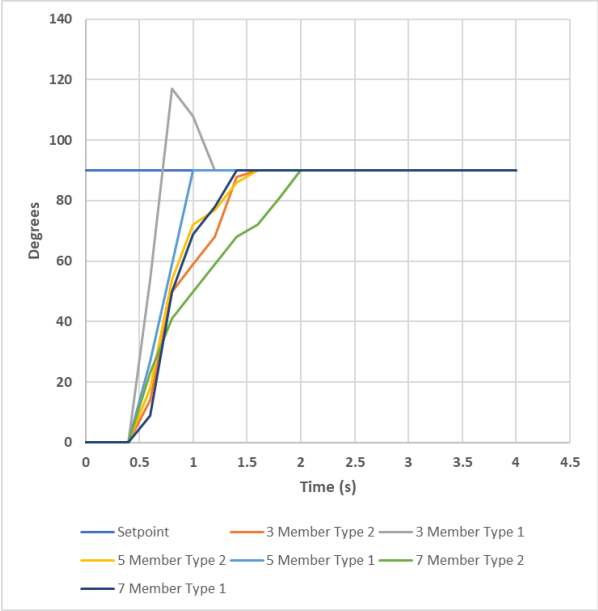

Fig. 12. Testing the steering rotation movement at 90 degrees.

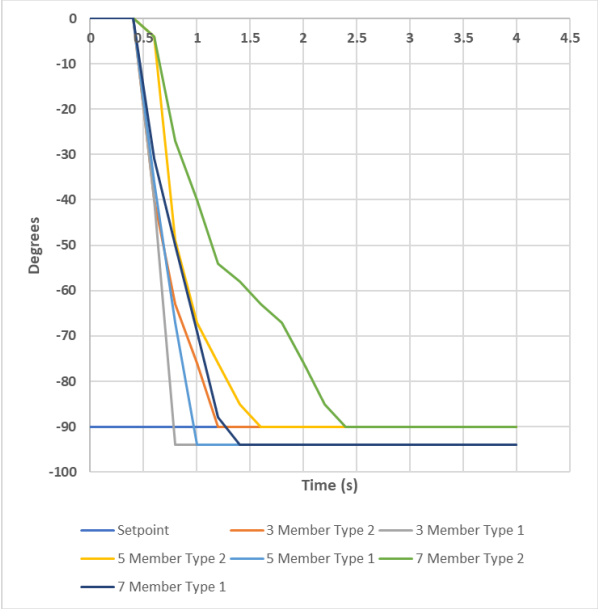

Fig. 13. Testing the steering rotation movement at -90 degrees.

Based on Fig. 15, each fuzzy logic method with 3, 5, and 7 members shows no overshoot. Both the response time and the settlement time are consistently long, ranging from 6.4 to 13.2 seconds. Regarding steady-state error, type-2 FLC performs better, especially with 3 and 5 members, where it equals the given set point. For type-1 FLC, there is still an error between 1 cm–2 cm. This steady-state error occurs in the Y-coordinate condition, providing good accuracy with an error value of 0.1 cm. However, in the X-coordinate, the error ranges from 0.5 cm to 3 cm.

The use of three membership functions results in a shorter rise time compared to other conditions. The use of 5 and 7 membership functions has a longer rise time than the condition with 3 members. In terms of stability, 7 memberships yield more stable results. In type-2 FLC, having upper and lower bounds makes its control results more stable because the input parameters have a tighter range, resulting in smaller crisp values. However, the process takes longer compared to the process carried out by type-1 FLC.

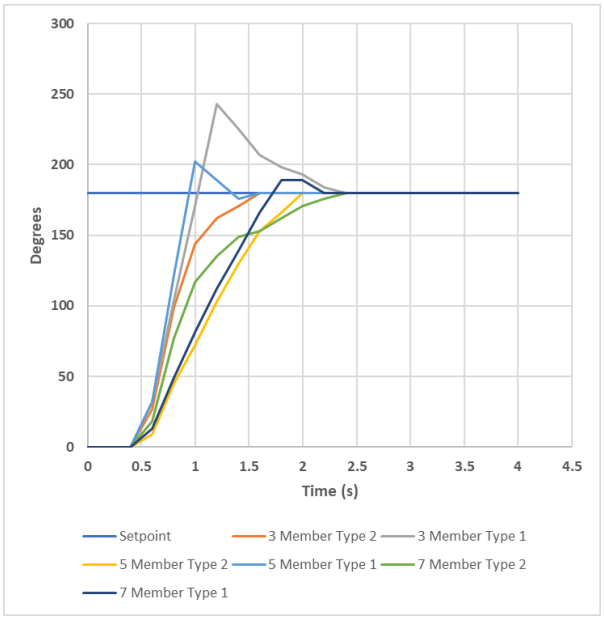

Fig. 14. Testing the steering rotation movement at 180 degrees.

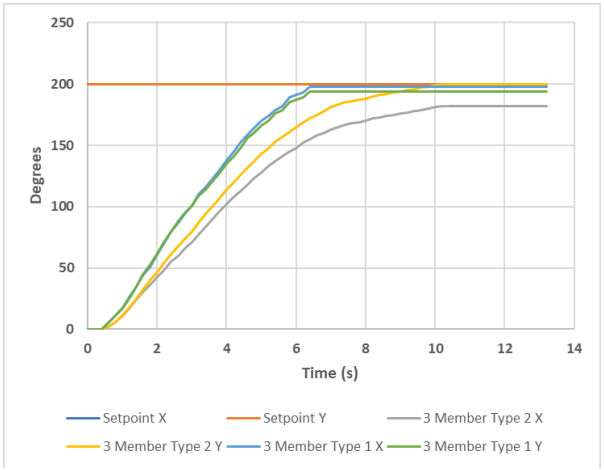

(a)

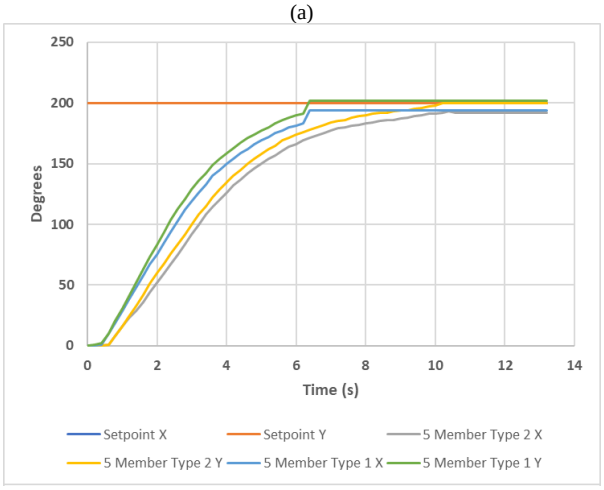

(b)

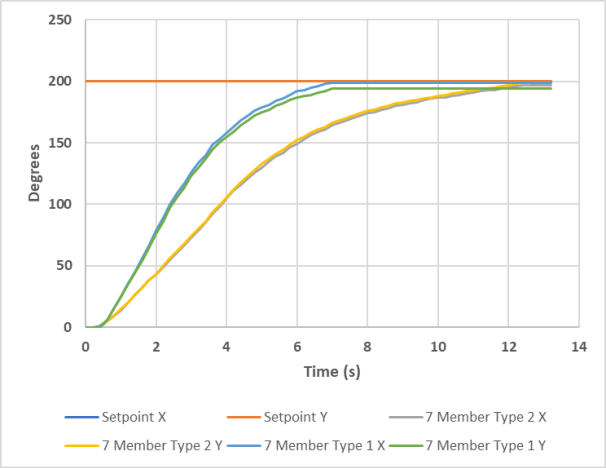

(c)

Fig. 15. Testing the XY-coordinate movement: (a) 3 memberships function; (b) 5 memberships function; (c) 7 memberships function.

Furthermore, as discussed in Fig. 5, it can be observed that in the type-2 FLC method, there is an additional reducer block, thus increasing the processing time. This is what makes the processing time of fuzzy logic type-2 slower. However, with good accuracy and stability factors, this controller can be considered as one of the controllers in a system, although further verification is needed in other studies.

VI. CONCLUSIONS

In this study, type-2 FLC is implemented in the swerve drive method to control the movement of a humanoid robot and is compared with type-1 FLC. As discussed in the results, type-2 FLC exhibits greater stability, minimal steady-state error, and no overshoot, but it has a longer response time and processing duration compared to type-1 FLC. The swerve drive method operates effectively by leveraging the collaboration of gears and direct current (DC) motors. Our future work will involve utilising this swerve drive method and type-2 FLC for the implementation of the humanoid robot's movement, particularly in navigating obstacles and assessing its ability to move smoothly.

CONFLICTS OF INTEREST

The authors declare that they have no conflicts of interest.

REFERENCES

[1] L. Tagliavini, G. Colucci, A. Botta, P. Cavallone, L. Baglieri, and G. Quaglia, "Wheeled mobile robots: State of the art overview and kinematic comparison among three omnidirectional locomotion strategies", *J. Intell. Robot. Syst.*, vol. 106, no. 3, p. 57, 2022. DOI: 10.1007/s10846-022-01745-7.

[2] E. H. Binugroho, A. Setiawan, Y. Sadewa, P. H. Amrulloh, K. Paramasastra, and R. W. Sudibyo, "Position and orientation control of three wheels swerve drive mobile robot platform", in *Proc. of 2021 International Electronics Symposium (IES)*, 2021, pp. 669–674. DOI: 10.1109/IES53407.2021.9593947.

[3] B. DeNoma, "4-wheel independent steering "swerve drive"", B.S. thesis, Department of Mechanical and Materials Engineering, College of Engineering and Applied Science, University of Cincinnati, 2022.

[4] J. Hu, "The chassis design of the Swerveomni directional wheel", *Acad. J. Eng. Technol. Sci.*, vol. 4, no. 5, pp. 24–30, 2021. DOI: 10.25236/AJETS.2021.040505.

[5] C. Dimoush, V. Ramanathan, C. Geyer, and W. Beaty, "Improved swerve drive design with suspension", Mechanical Engineering Design Project Program, The University of Texas at Austin, Austin, Texas 2020.

[6] A. Setiwan, M. I. Faisal, E. H. Binugroho, H. S. Maulana, N. F. Satria, and R. S. Dewanto, "Design and fabrication of swerve drive mechanism for mobile robot platform", in *Proc. of 2023 International Electronics Symposium (IES)*, 2023, pp. 348–353.

[7] R. Dhelika, A. F. Hadi, and P. A. Yusuf, "Development of a motorized hospital bed with swerve drive modules for holonomic mobility", *Appl. Sci.*, vol. 11, no. 23, p. 11356, 2021. DOI: 10.3390/app112311356.

[8] B. DeNoma, M. Kendall, N. Poulos, J. Dong, and R. Frank, "Four-wheel independent steering swerve drive for First Robotics Competition", in *Proc. of ASME 2022 International Mechanical Engineering Congress and Exposition*, 2022, pp. 1–8, vol. 5. DOI: 10.1115/IMECE2022-96192.

[9] K. Khairnar, M. Gavani, and S. Nalawade, "Design and control of swerve drive robot using kinematic model", in *Proc. of 2023 14th International Conference on Computing Communication and Networking Technologies (ICCCNT)*, 2023, pp. 1–5. DOI: 10.1109/ICCCNT56998.2023.10307118.

[10] R. Davnall, "Solving the single-vehicle self-driving car trolley problem using risk theory and vehicle dynamics", *Sci. Eng. Ethics*, vol. 26, no. 1, pp. 431–449, 2020. DOI: 10.1007/s11948-019-00102-6.

[11] N. M. Pawar and N. R. Velaga, "Effect of time pressure on steering control of the drivers in a car-following situation", *Transp. Res. Part F: Traffic Psychol. Behav.*, vol. 80, pp. 218–236, 2021. DOI: 10.1016/j.trf.2021.04.007.

[12] R. Lawlor, "The ethics of automated vehicles: Why self-driving cars should not swerve in dilemma cases", *Res Publica*, vol. 28, no. 1, pp. 193–216, 2022. DOI: 10.1007/s11158-021-09519-y.

[13] B. Meder, N. Fleischhut, N.C. Krumnau, and M. R. Waldmann, "How should autonomous cars drive? A preference for defaults in moral judgments under risk and uncertainty", *Risk Anal.*, vol. 39, no. 2, pp. 295–314, 2019. DOI: 10.1111/risa.13178.

[14] D. Pratama, E. H. Binugroho, and F. Ardilla, "Movement control of two wheels balancing robot using cascaded PID controller", in *Proc. of 2015 International Electronics Symposium (IES)*, 2015, pp. 94–99. DOI: 10.1109/ELECSYM.2015.7380821.

[15] Y. Ye, C.-B. Yin, Y. Gong, and J.-j. Zhou, "Position control of nonlinear hydraulic system using an improved PSO based PID controller", *Mech. Syst. Signal Process.*, vol. 83, pp. 241–259, 2017. DOI: 10.1016/j.ymssp.2016.06.010.

[16] M. A. E. Mohamed El-Saeed, A. F. Abdel-Gwaad, and M. A. Farahat, "Capacitor Allocation Using Multiobjective Water Cycle Algorithm and Fuzzy Logic", *Elektron Elektrotech*, vol. 28, no. 2, pp. 35-45, 2022. DOI: 10.5755/j02.eie.30355.

[17] R. R. Bambulkar, G. S. Phadke, and S. Salunkhe, "Movement control of robot using fuzzy PID algorithm", in *Proc. of 3rd International Conference on Electrical, Electronics, Engineering Trends, Communication, Optimization and Sciences (EEECOS 2016)*, 2016, pp. 1–5. DOI: 10.1049/cp.2016.1519.

[18] H. Chaudhary, V. Panwar, R. Prasad, and N. Sukavanam, "Adaptive neuro fuzzy based hybrid force/position control for an industrial robot manipulator", *J. Intell. Manuf.*, vol. 27, pp. 1299–1308, 2016. DOI: 10.1007/s10845-014-0952-1.

[19] O. Castillo, L. Amador-Angulo, J. R. Castro, and M. Garcia-Valdez, "A comparative study of type-1 fuzzy logic systems, interval type-2 fuzzy logic systems and generalized type-2 fuzzy logic systems in control problems", *Inf. Sci.*, vol. 354, pp. 257–274, 2016. DOI: 10.1016/j.ins.2016.03.026.

[20] D. Wu and W. W. Tan, "A type-2 fuzzy logic controller for the liquid-level process", in *Proc. of 2004 IEEE International Conference on Fuzzy Systems (IEEE Cat. No. 04CH37542)*, 2004, pp. 953–958, vol. 2. DOI: 10.1109/FUZZY.2004.1375536.

[21] O. Castillo and P. Melin, "A review on interval type-2 fuzzy logic applications in intelligent control", *Inf. Sci.*, vol. 279, pp. 615–631, 2014. DOI: 10.1016/j.ins.2014.04.015.

[22] R. L. McCoy, "Six-degrees-of-freedom (6 DOF) and modified point-mass trajectories", *Mod. Exter. Ballist. Launch Flight Dyn. Symmetric Proj.*, pp. 187–212, 1999.

[23] L. C. Hainz III and M. Costello, "Modified projectile linear theory for rapid trajectory prediction", *J. Guid. Control. Dyn.*, vol. 28, no. 5, pp. 1006–1014, 2005. DOI: 10.2514/1.8027.

[24] M. Vukobratović, B. Borovac, and M. Raković, "Comparison of PID and fuzzy logic controllers in humanoid robot control of small disturbances", in *Research and Education in Robotics — EUROBOT*

2008. EUROBOT 2008. Communications in Computer and Information Science, vol. 33. Springer, Berlin, Heidelberg, 2009, pp. 42–53. DOI: 10.1007/978-3-642-03558-6_5.

[25] O. Castillo, P. Melin, J. Kacprzyk, and W. Pedrycz, "Type-2 fuzzy logic: Theory and applications", in *Proc. of 2007 IEEE International Conference on Granular Computing (GRC 2007)*, 2007, pp. 145–145. DOI: 10.1109/GrC.2007.118.

[26] N. N. Karnik, J. M. Mendel, and Q. Liang, "Type-2 fuzzy logic systems", *IEEE Trans. Fuzzy Syst.*, vol. 7, no. 6, pp. 643–658, 1999. DOI: 10.1109/91.811231.